Proceedings of CONF-MCEE 2027 Symposium: Advanced Nanomaterials and 2D Materials: Synthesis, Modeling, and Applications
DOI: 10.54254/2755-2721/2027.AD37462

Recent Progress in Photochromic Molecules and Their Application in Organic Field Effect Transistors

Xiaoyu Liu

School of Science, Tianjin University, Tianjin, China
3023210034@tju.edu.cn

Abstract. This paper reviews recent progress in the integration of photochromic molecules into organic field-effect transistors (OFETs). Three major classes of photoresponsive units—diarylethene (DAE), spiropyran (SP), and azobenzene (AZO)—are highlighted for their incorporation into channel, electrode, and dielectric layers of OFETs, enabling light-controlled modulation of photoelectric properties. These hybrid devices show promise in optical memories, photonic logic circuits, multi-stimuli-responsive sensors, and flexible electronics. This review systematically summarizes the fabrication methodologies for introducing photochromic moieties into OFET components, followed by a detailed evaluation of device performance, including electrical characteristics, photosensitivity, and other functional attributes. The underlying working mechanisms, particularly the structure–property correlations governing photoresponse, are briefly discussed. Despite substantial advances, several critical challenges persist, including photobleaching degradation, limited response kinetics, insufficient operational stability, and difficulties in scalable manufacturing. This paper concludes with an in-depth analysis of these bottlenecks and offers forward-looking perspectives on possible solutions and future research directions for photochromic molecule-functionalized OFETs. Emphasis is placed on molecular design strategies, interface engineering, and device architecture optimization as key pathways toward practical applications.

Keywords: Photochromic molecules, Organic field-effect transistors, Diarylethene, Spiropyran, Azobenzene

1. Introduction

Organic field-effect transistors (OFETs) have become a key technology in modern electronics due to their flexibility, solution processability, large-area fabrication, and cost-effectiveness [1]. Beyond conventional switching, OFET platforms have enabled diverse functions including memory [2], gas sensing [3], and neuromorphic simulation [4]. Among functionalized OFETs, organic phototransistors have attracted particular attention for their light-responsive capability, which is essential for photodetectors [5], optical memory [6], and logic circuits [7].

A feasible strategy to construct organic phototransistors is the direct incorporation of photochromic molecules into OFETs [8]. These molecules undergo reversible structural changes upon light irradiation, allowing precise electrical modulation. Research on this phenomenon began

© 2026 The Authors. This is an open access article distributed under the terms of the Creative Commons Attribution License 4.0 (https://creativecommons.org/licenses/by/4.0/).

DOI: 10.54254/2755-2721/2027.AD37462

with Hirshberg in 1956 [9], and over nearly seven decades, photochromic compounds have shown versatility in smart textiles [10], photocatalysis [11], and other fields. Their excellent photosensitivity in devices offers clear advantages over conventional OFETs that rely on trap states for light detection [12]. This review examines recent progress in photochromic OFETs, focusing on incorporation strategies, mechanisms, and device performance.

2. Structure of OFET and photochromic groups

A conventional OFET is a three-terminal device comprising a semiconductor (active) layer, a dielectric (gate insulator) layer, and source/drain/gate electrodes. Based on layer stacking order, OFETs are classified into four architectures: bottom-contact/bottom-gate, bottom-contact/top-gate, top-contact/bottom-gate, and top-contact/top-gate (Figure 1). Self-assembled monolayers (SAMs) are commonly used to modify dielectric and electrode interfaces for improved charge transport [13].

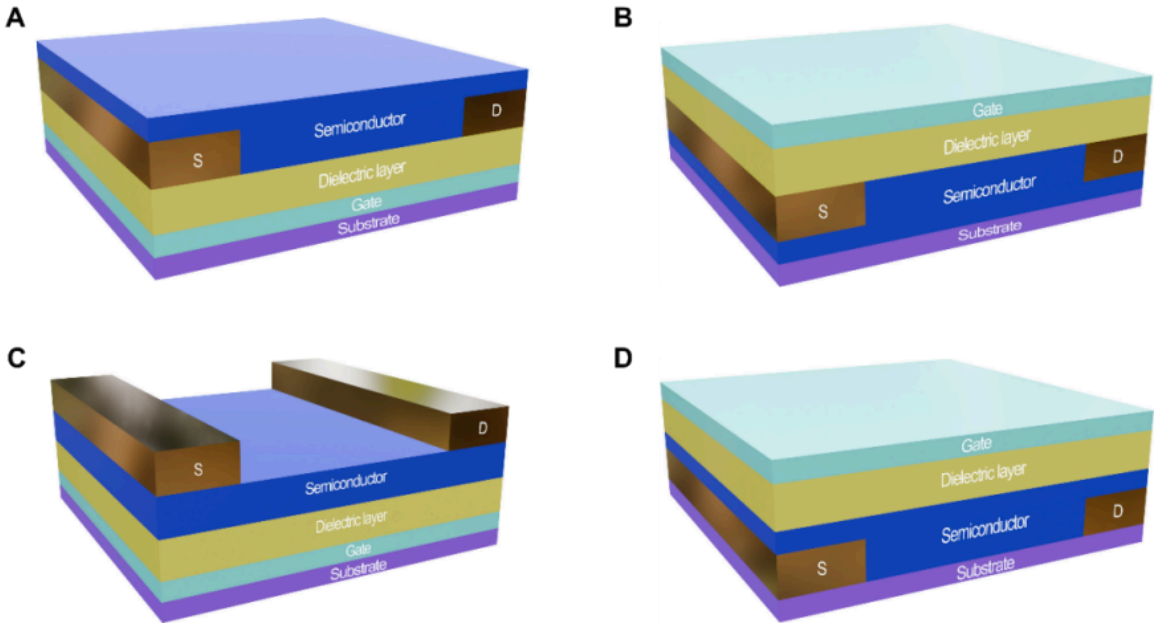

Figure 1. Different architectures of OFETs. (A) bottom contact and bottom gate. (B) bottom contact and top gate. (C) top contact and bottom gate. (D) top contact and top gate

Device operation relies on gate-voltage-induced charge accumulation at the dielectric–semiconductor interface. Key performance metrics include threshold voltage (VT), on/off ratio (Ion/Ioff), and mobility (μ). For photoresponsive devices, additional figures of merit are defined: photosensitivity (P), photoresponsivity (R in A/W), and specific detectivity (D* in Jones), calculated as follows [14]:

$$P = \frac{|I_{light} - I_{dark}|}{I_{dark}} \text{ or } \frac{|I_{UV} - I_{Vis}|}{I_{Vis}} \quad (1)$$

$$R = \frac{|I_{light} - I_{dark}|}{P_{ill}} \text{ or } \frac{|I_{UV} - I_{Vis}|}{P_{ill}} \quad (2)$$

$$D^* = \frac{R}{\sqrt{2qJ_{dark}}} \quad (3)$$

DOI: 10.54254/2755-2721/2027.AD37462

Where Ilight/Idark and IUV/IVis are source-drain currents under illumination/dark and UV/visible light, respectively, Pill is optical power density, q is the elementary charge, and Jdark is dark current density.

Photochromic molecules undergo reversible isomerization upon specific light irradiation, accompanied by color changes [8]. In OFET applications, three classes dominate: diarylethene (DAE), spiropyran (SP), and azobenzene (AZO) (Figure 2). These molecules can function as independent light-sensitive dopants in non-photoisomerizable matrices or be covalently incorporated into small molecules/polymers to create novel photochromic materials, enabling tunable functionalities across various device layers. Figure 2 summarizes the molecules discussed in this review.

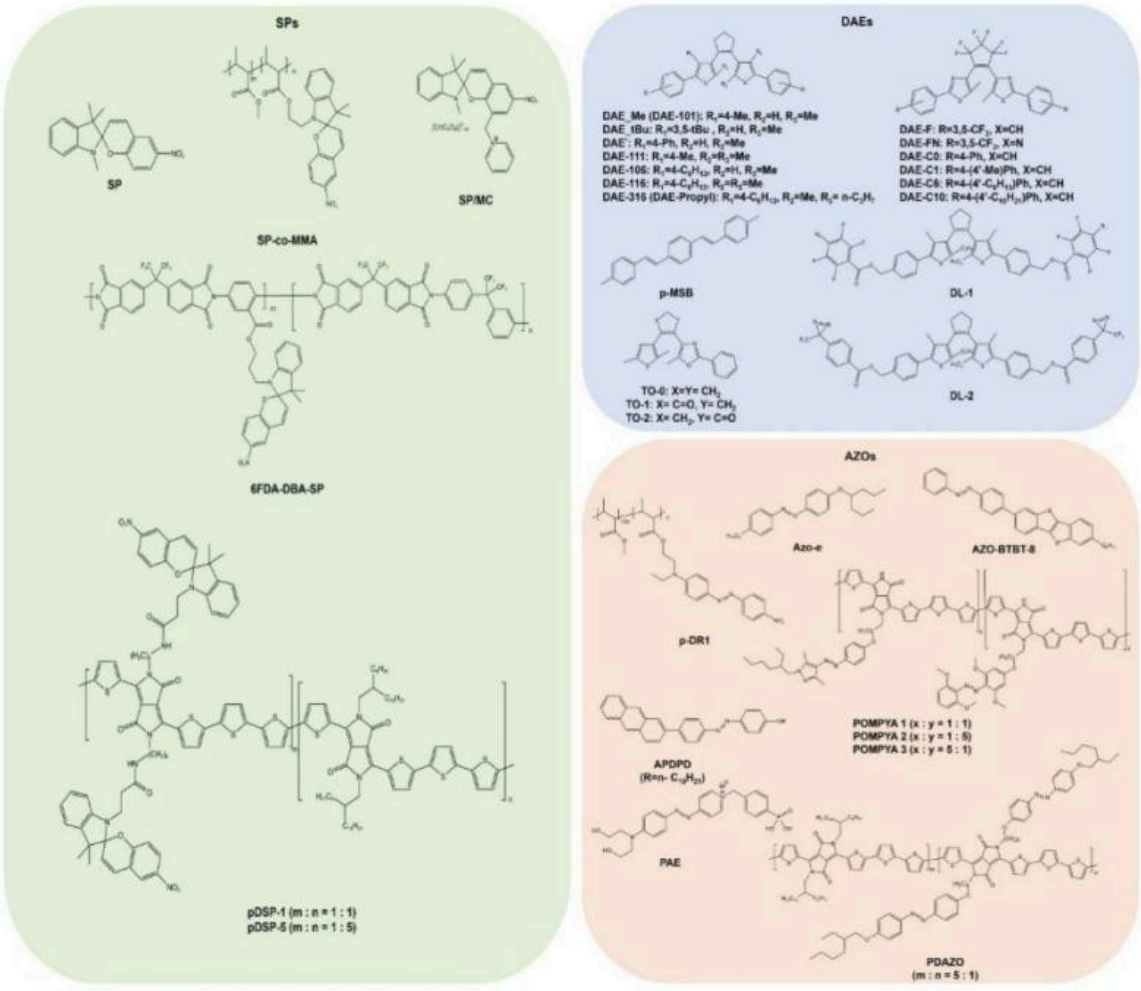

Figure 2. Chemical structures of representative photochromic molecules

DOI: 10.54254/2755-2721/2027.AD37462

3. Photochromic channel

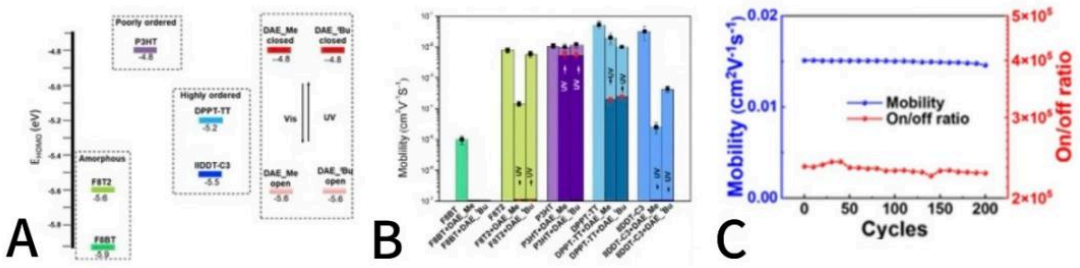

Figure 3. (A) HOMO energy levels of F8BT, F8T2, P3HT, DPPT-TT, IIDDT-C3, DAE_Me and DAE_tBu (B) Mobility of devices based on polymers/DAE matrices. (C) Mobility and on/off ratio varying curve after bending cycles [15, 16]

Channel engineering offers the most direct route to optical control, via either blending or covalent incorporation of photochromic molecules.

Hou et al. blended two DAE derivatives with five polymer semiconductors (Figure 3) [15]. DAE photoisomerization depends strongly on polymer matrix order: crystalline polymers constrain DAEs and favor UV cyclization, while amorphous matrices allow free switching. Energy-level alignment is critical—when polymer HOMO lies below open-form DAE HOMO, permanent hole trapping occurs. DPPT-TT/DAE_tBu achieved the highest mobility (0.01 $cm^2 V^{-1} s^{-1}$), while F8T2/DAE_tBu gave Ion/Ioff >10^3 [15].

Li et al. synthesized AZO-BTBT-8 with an AZO group on the BTBT backbone [16]. Light-induced self-strained engineering enables reversible mobility switching: from 0.23 to 3.80 $cm^2 V^{-1} s^{-1}$ on Si, and 0.015 to 0.141 $cm^2 V^{-1} s^{-1}$ on PET, stable after 200 bending cycles [16].

4. Photochromic functionalized electrode

Table 1. Electrical properties of OFETs

Material	Semiconductor	Dielectric	μ ($cm^2 V^{-1} s^{-1}$)	I_{on}/I_{off}	V_{th}(V)	Ref.
DAE SAM†	P(NDI2O-T2)	Cytop	0.1(o-DAE)	10^5-10^6	-3.10	[40]
SP-SH SAM	Pentacene	SiO_2/Si	0.02	1×10^5 ‡	N/A	[41]
AZO SAM†	PDIF-CN_2	HMDS/ SiO_2/Si	8.3×10^{-3}	N/A	-3.8	[14]

Table 1 shows summaries of electrical properties of OFETs using photochromic functionalized electrodes, but there are no intact molecules in SAM, and no specific abbreviations were used in the original article. Therefore, it is named after its main molecular types. These data are estimated based on charts from original articles. N/A means not found in the article. Surface functionalization represents a powerful strategy for modulating interfacial properties in OFETs [18]. Specific molecules can form self-assembled monolayers (SAMs) to functionalize the metal source-drain electrodes. The formation of SAMs on metal electrodes enables precise control over the charge injection and extraction processes occurring at the electrode–semiconductor interface [19]. It is possible for SAMs to tune the work function of metal electrodes by introducing a dipole facing the metal or by inducing a shift of the Fermi level, both of which contribute to changes in metal work

DOI: 10.54254/2755-2721/2027.AD37462

function [20]. Building on these principles, the development of photosensitive electrode functionalization layers offers a promising avenue for optically tunable transistors. However, this approach requires top-contact architectures and careful channel material selection to avoid spectral interference.

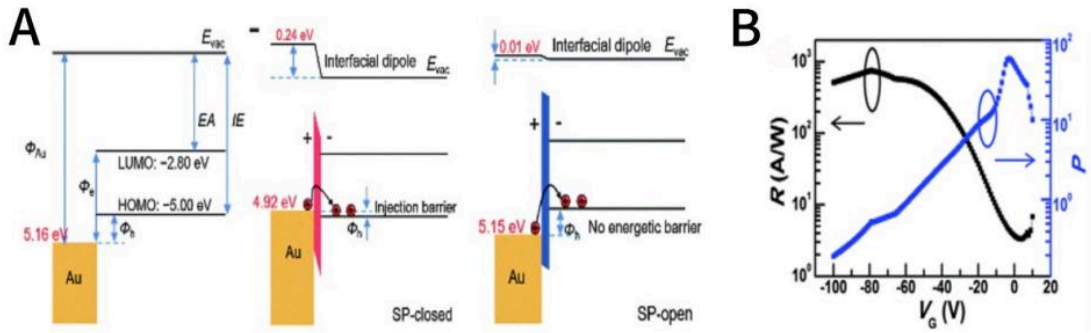

Figure 4. (A) Energy level diagrams of working function of Au (ΦAu), HOMO and LUMO energy levels of pentacene, pristine injection barrier of electrons (Φe) and holes (Φh). (B) Responsivity (R)-gate voltage curve and photosensitivity (P)-gate voltage curve (VD = -100 V). Effective irradiance power: 7.4 mW cm-2 [17]

A pioneering and representative study in this area was reported by Zhang et al. in 2016, who integrated spiropyran (SP) moieties for functionalizing source and drain electrodes (Figure 4) [17]. As discussed previously, the SP group exhibits a light-responsive tunable dipole moment, which, when coupled with metal electrodes, enables precise work function modulation. To achieve this, the researchers synthesized an alkanethiol-terminated SP derivative (SP-SH) specifically designed for Au electrode conjugation, distinct from the N-alkane spiropyran variants used in channel materials. A dodecanethiol chain serves as the molecular bridge between the SP group and the gold surface. The dodecanethiol group cannot undergo the photochromic process; thus, the light-triggered effect is mainly produced by the SP group. This process dynamically alters both the orientation and magnitude of the dipole moment within the SAM layer, thereby inducing reversible changes in the Au–SAM interface work function. The HOMO energy level of the p-type semiconductor (pentacene in this case) is −5.00 eV. The closed-form SP lowers the work function to 4.92 eV, creating an injection barrier and resulting in high contact resistance. By contrast, open-form SP lowers the work function to 5.15 eV, allowing the hole injection process to proceed with no energetic barrier, resulting in low contact resistance. The devices fabricated in this way show good performance in both electronic properties and photoswitching. Device mobility is measured to be 0.02 $cm^2 V^{-1} s^{-1}$, and the photosensitivity (P) and photoresponsivity (R) reach ~60 and ~800 A W^{-1}, respectively. This represents a substantial enhancement over pristine pentacene devices, particularly in photodetection performance [17].

5. Photochromic self-assembled monolayer on dielectric and photochromic dielectric layer

5.1. Photochromic SAM on dielectric

The key to the photochromic SAM strategy lies at the dielectric/semiconductor interface. A layer of photochromic molecules (e.g., azobenzene, spiropyran, or diarylethene) is covalently anchored to the gate dielectric surface. These molecules undergo reversible photoisomerization upon exposure to light of specific wavelengths (e.g., trans–cis transition for AZO, open/closed ring for SP, or ring-

DOI: 10.54254/2755-2721/2027.AD37462

open/ring-close for DAE). This isomerization greatly changes the molecular dipole moments and the molecular packing at the interfaces. The resulting surface electrostatic environment changes directly modulate the charge carrier density in the upper semiconductor channel, effectively changing the threshold voltage of the transistor. This light-induced threshold voltage shift produces a nonvolatile memory effect that enables data states to be optically written and erased in OFET memories [21].

A representative and impactful work in this area was reported by Professor Guo Xuefeng's team at Peking University [21]. They modified DAE as a self-assembled single-molecular layer (SAM) on the dielectric layer of hafnium dioxide (HfO_2) to form a photoactive hybrid bilayer dielectric (Figure 5). The energy level changes of DAE affect the tunneling energy barrier of photogenerated electrons at the interface, thereby achieving charge capture and release. The device uses optical signals for writing and erasing with electrical signals for readout, showing large, reversible threshold voltage drift, long retention time, and good nonvolatile signal processing capabilities, successfully implementing nonvolatile optical memory functions [21].

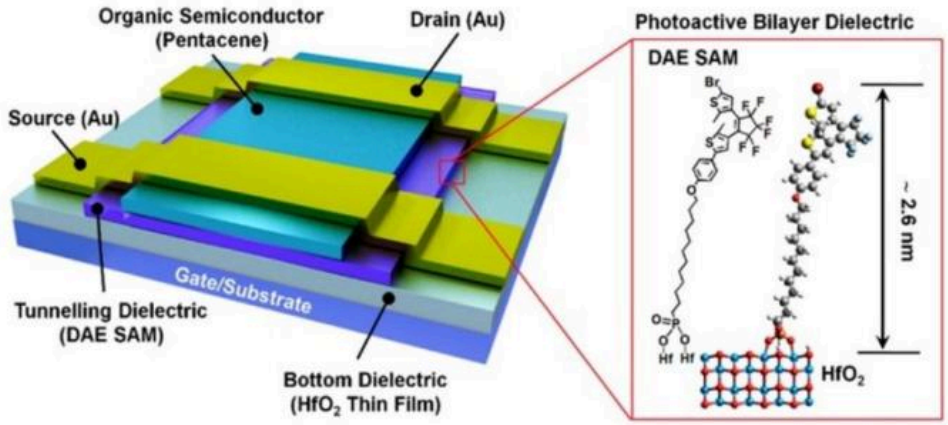

Figure 5. Schematic cross section of a PHBD OMT

5.2. Photochromic dielectric layer

The photochromic dielectric layer is another key component that imparts photoresponsiveness to OFETs and enables multifunctional optoelectronic characteristics. Its core principle is to use photochromic materials that undergo reversible isomerization under specific wavelength light, causing significant changes in molecular configuration, dipole moment, and electron energy levels, thereby modulating the capacitance characteristics of the dielectric layer or the charge behavior at the dielectric/semiconductor interface, ultimately achieving optical regulation of the transistor threshold voltage and channel current. The photochromic dielectric layer mainly realizes functional regulation through two mechanisms.

5.2.1. Dipole mechanism

SP shows a large dipole increase from closed (≈5.4 D) to open (≈11 D) forms. Collective dipole changes in the dielectric generate a polarization field that modulates channel carrier density, analogous to an applied gate bias, causing VT drift.

A representative study employing this mechanism was conducted by Lutsyk et al., who constructed an n-type organic field-effect transistor with a dielectric layer composed of spiropyran

DOI: 10.54254/2755-2721/2027.AD37462

(SP) molecules dispersed in a polymethyl methacrylate (PMMA) matrix [22]. SP molecules undergo a ring-opening reaction under ultraviolet (UV) light irradiation and convert to the merocyanine (MR) form with a significantly higher dipole moment (SP ~5.4 D, MR ~11 D); under visible light irradiation or thermal relaxation, MR reversibly returns to the SP form. This photochromic reaction causes a reversible change in the dielectric constant. Their results show that after UV illumination, the threshold voltage decreases (from 34 V to 29 V) and the source-drain current increases; the threshold voltage and current can be restored to the initial state through thermal relaxation or visible light exposure (Figure 6) [22]. This work demonstrates that reversible modulation of dielectric layer capacitance can be achieved through photo-controlled dipole moment changes, providing an important basis for the development of organic optoelectronic devices with reversible and lossless regulation.

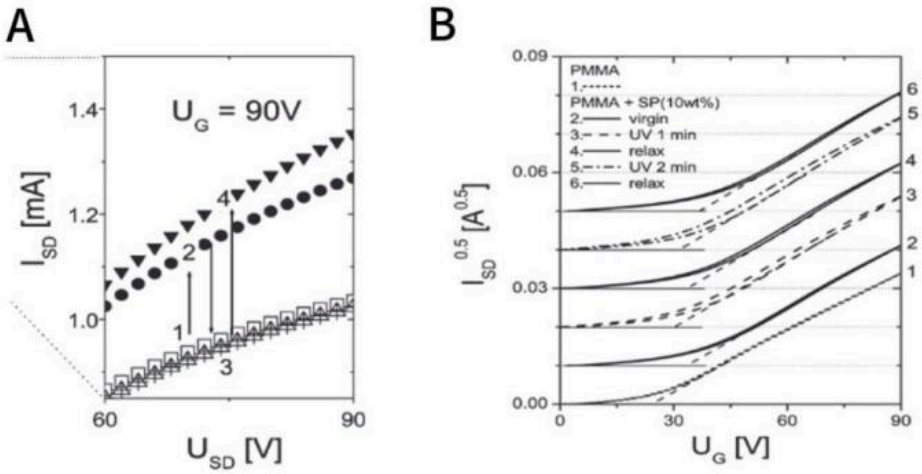

Figure 6. (A) UG = 90 V showing the switching cycle. (B) Locus (USD = UG) current-voltage characteristics for PMMA/P13 (curve 1) and (PMMA þ SP)(10 wt %)/P13 FETs (curves 2-6)

5.2.2. Charge trapping mechanism

DAE closed-ring isomers have deeper HOMO levels due to extended π-conjugation, introducing reversible hole traps that capture carriers and modulate current.

A representative study of this mechanism was reported by Gemayel et al., who prepared photo-switchable transistors by blending two different alkyl-substituted DAE photochromic molecules—DAE_Me (methyl substituted) and DAE_tBu (tert-butyl substituted)—with organic semiconductors at a 20 wt% ratio, and systematically studied the relationship between interface interaction, energy level matching, and charge trapping behavior [23]. Two semiconductor matrices were selected: polymer semiconductor P3HT and high-performance small-molecule semiconductor C_{12}-BTBT. The results show that DAE molecules undergo open-loop/closed-loop isomerization under light, and their HOMO energy level changes significantly (open-loop HOMO is shallow, closed-loop HOMO becomes deeper), thereby introducing reversible hole trap energy levels into the semiconductor matrix. When DAE is in the closed-loop state, its HOMO energy level is lower than that of the semiconductor matrix, effectively capturing holes and causing the device current to drop; in the open-loop state, the trap energy level disappears and the current recovers. The study further found that the alkyl substituent design of DAE can effectively regulate its compatibility and phase separation behavior with the semiconductor matrix: DAE_tBu is better compatible with BTBT and

DOI: 10.54254/2755-2721/2027.AD37462

hardly destroys the crystalline nature of BTBT, so the device maintains high mobility (>0.2 $cm^2 V^{-1} s^{-1}$) in the dark state while achieving ~40% photocurrent modulation (Figure 7) [23]. This work reveals that optimizing energy level alignment and morphology control at the photochromic molecule–semiconductor interface through molecular design is key to achieving efficient, reversible photo-controlled charge trapping and nonvolatile photomemory functions.

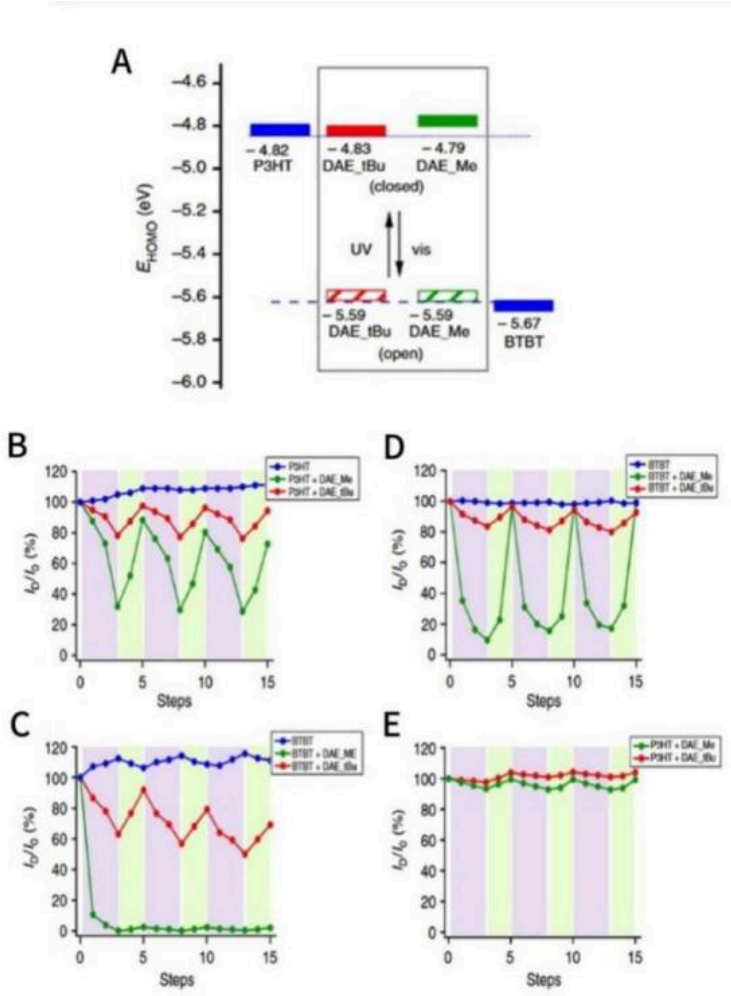

Figure 7. (A) Energy level diagram illustrating HOMO alignment between semiconductors and DAEs in open/closed forms. (B–E) Reversible photoswitching cycles of normalized drain current under UV (365 nm) and visible (546 nm) light [23]

6. Conclusion

This review summarizes recent progress in the integration of photochromic molecules into organic field-effect transistors (OFETs), with particular emphasis on diarylethene (DAE), spiropyran (SP), and azobenzene (AZO) systems. Different strategies for introducing photochromic functionalities into OFETs have been discussed, including their incorporation into semiconductor channels, source/drain electrodes, and dielectric layers. The corresponding photoresponse mechanisms, such as light-induced changes in molecular conformation, energy-level alignment, electrode work function, dipole moment, and charge-trapping behavior, have also been reviewed. These approaches enable reversible modulation of mobility, VT, and drain current for applications in memory, sensing,

DOI: 10.54254/2755-2721/2027.AD37462

logic, and flexible electronics. Key challenges remain: photofatigue, slow switching kinetics, limited stability, and scalability. Future work should focus on fatigue-resistant molecules, faster switching, interface engineering, and device optimization to enable practical applications in low-power storage, sensing, neuromorphic computing, and wearable electronics.

References

[1] Newman, C. R., Frisbie, C. D., da Silva, D. A., Brédas, J. L., Ewbank, P. C., & Mann, K. R. (2004). Introduction to organic thin film transistors and design of n-channel organic semiconductors. *Chemistry of Materials, 16*(23), 4436–4451. DOI: 10.1021/cm049391x.

[2] Lin, Y. C., Yang, W. C., Chiang, Y. C., & Chen, W. C. (2022). Recent advances in organic phototransistors: Nonvolatile memory, artificial synapses, and photodetectors. *Small Sci, 2*(4), 2100109. DOI: 10.1002/smsc.202100109.

[3] Mun, S., Park, Y., Lee, Y. E. K., & Sung, M. M. (2017). Highly sensitive ammonia gas sensor based on single-crystal poly(3-hexylthiophene) (P3HT) organic field effect transistor. *Langmuir, 33*(47), 13554–13560. DOI: 10.1021/acs.langmuir.7b02466.

[4] Chen, Y., Han, B., Gobbi, M., Hou, L., & Samori, P. (2025). Responsive molecules for organic neuromorphic devices: Harnessing memory diversification. *Adv Mater, 37*(19), e2418281. DOI: 10.1002/adma.202418281.

[5] Jung, M. J., Kim, Y., Baeg, K. J., & Lee, E. K. (2025). Ultraviolet photodetector fabrication with low-power dissipation based on organic suboptimal source-gated transistor architecture and MoO_3-doped pentacene. *Small, 21*(2). DOI: 10.1002/smll.202408772.

[6] Bai, S. L., Haase, K., Hambsch, M., & Mannsfeld, S. C. B. (2025). Organic multibit phototransistor memories with high external quantum efficiency. *Advanced Electronic Materials, 11*(2). DOI: 10.1002/aelm.202400307.

[7] Yan, Y. K., Wu, Y. J., Shao, L., Yang, L. F., Wu, Z., Li, W. H., Yi, Z. R., Liu, Y. Q., & Zhao, Y. (2022). An OFET-based involutive logic circuit with wide-range threshold shift compensability. *Advanced Electronic Materials, 8*(10). DOI: 10.1002/aelm.202200442.

[8] Xu, C., Zhang, J., Xu, W., & Tian, H. (2021). Multifunctional organic field effect transistors constructed with photochromic molecules. *Materials Chemistry Frontiers, 5*(3), 1060–1075. DOI: 10.1039/d0qm00567c.

[9] Hirshberg, Y. (1956). Reversible formation and eradication of colors by irradiation at low temperatures. A photochemical memory model. *Journal of the American Chemical Society, 78*(10), 2304–2312. DOI: 10.1021/ja01591a075.

[10] Zhang, H. Y., Fan, J., Cheng, H. Y., Yu, D., & Wang, W. (2024). High optical contrast, dual-responsive, wearable photochromic fibers for smart textile engineering. *Surfaces and Interfaces, 51*. DOI: 10.1016/j.surfin.2024.104795.

[11] Singh, A., Verma, P., Samanta, D., Dey, A., Dey, J., & Maji, T. K. (2021). Stabilization of ultra-small gold nanoparticles in a photochromic organic cage: Modulating photocatalytic CO_2 reduction by tuning light irradiation. *Journal of Materials Chemistry A, 9*(9), 5780–5786. DOI: 10.1039/d0ta12195a.

[12] Liu, J., Jiang, L., Shi, J., Li, C., Shi, Y., Tan, J., Li, H., Jiang, H., Hu, Y., Liu, X., et al. (2020). Relieving the photosensitivity of organic field-effect transistors. *Adv Mater, 32*(4), e1906122. DOI: 10.1002/adma.201906122.

[13] Sinha, S., Wang, C. H., Islam, A., Yang, Y. W., & Mukherjee, M. (2012). Improvement of rubrene thin film transistor with self assembled monolayer of octadecyltrichlorosilane (OTS). In *56th DAE-Solid State Physics Symposium (SSPS), SRM Univ, Kattankulathur, INDIA, Dec 19-23, 2011 (Vol. 1447)*, pp. 977-+. DOI: 10.1063/1.4710331.

[14] Yao, Y., Chen, Y., Wang, H., & Samorì, P. (2020). Organic photodetectors based on supramolecular nanostructures. *Smartmat, 1*(1). DOI: 10.1002/smm2.1009.

[15] Hou, L. L., Leydecker, T., Zhang, X. Y., Rekab, W., Herder, M., Cendra, C., Hecht, S., McCulloch, I., Salleo, A., Orgiu, E., et al. (2020). Engineering optically switchable transistors with improved performance by controlling interactions of diarylethenes in polymer matrices. *Journal of the American Chemical Society, 142*(25), 11050–11059. DOI: 10.1021/jacs.0c02961.

[16] Li, M., Zheng, J., Wang, X., Yu, R., Wang, Y., Qiu, Y., Cheng, X., Wang, G., Chen, G., Xie, K., et al. (2022). Light-responsive self-strained organic semiconductor for large flexible OFET sensing array. *Nature Communications, 13*(1), Article. DOI: 10.1038/s41467-022-32647-9.

[17] Zhang, H., Chen, H., Ma, W., Hui, J., Meng, S., Xu, W., Zhu, D., & Guo, X. (2016). Photocontrol of charge injection/extraction at electrode/semiconductor interfaces for high-photoresponsivity organic transistors. *Journal of Materials Chemistry C, 4*(23), 5289–5296, Article. DOI: 10.1039/c6tc00387g.

DOI: 10.54254/2755-2721/2027.AD37462

[18] Mosciatti, T., Greco, P., Leydecker, T., Eredia, M., Biscarini, F., & Samorì, P. (2017). Asymmetric injection in organic transistors via direct SAM functionalization of source and drain electrodes. *ACS Omega, 2*(7), 3502–3508. DOI: 10.1021/acsomega.7b00690.

[19] Youn, J., Dholakia, G. R., Huang, H., Hennek, J. W., Facchetti, A., & Marks, T. J. (2012). Influence of thiol self-assembled monolayer processing on bottom-contact thin-film transistors based on n-type organic semiconductors. *Advanced Functional Materials, 22*(9), 1856–1869. DOI: 10.1002/adfm.201102312.

[20] de Boer, B., Hadipour, A., Mandoc, M. M., van Woudenbergh, T., & Blom, P. W. M. (2005). Tuning of metal work functions with self-assembled monolayers. *Adv Mater, 17*(5), 621–+. DOI: 10.1002/adma.200401216.

[21] Chen, H., Cheng, N., Ma, W., Li, M., Hu, S., Gu, L., Meng, S., & Guo, X. (2016). Design of a photoactive hybrid bilayer dielectric for flexible nonvolatile organic memory transistors. *ACS Nano, 10*(1), 436–445. DOI: 10.1021/acsnano.5b05313 (acccessed 2025/08/20/17:36:28).

[22] Lutsyk, P., Janus, K., Sworakowski, J., Generali, G., Capelli, R., & Muccini, M. (2011). Photoswitching of an n-type organic field effect transistor by a reversible photochromic reaction in the dielectric film. *J. Phys. Chem. C, 115*(7), 3106–3114. DOI: 10.1021/jp108982x (acccessed 2025/08/20/17:36:23).

[23] Gemayel, M. E., Börjesson, K., Herder, M., Duong, D. T., Hutchison, J. A., Ruzié, C., Schweicher, G., Salleo, A., Geerts, Y., Hecht, S., et al. (2015). Optically switchable transistors by simple incorporation of photochromic systems into small-molecule semiconducting matrices. *Nature Communications, 6*(1), 6330. DOI: 10.1038/ncomms7330 (acccessed 2025/08/29/16:28:58).